

# Lawrence Berkeley National Laboratory

## Recent Work

### **Title**

SUBSTRUCTURE AND MECHANICAL PROPERTIES OF TD-NICKEL

### **Permalink**

<https://escholarship.org/uc/item/1sq4905z>

### **Authors**

Heimendahl, M. von  
Thomas, G.

### **Publication Date**

1964-02-01

**University of California**  
**Ernest O. Lawrence**  
**Radiation Laboratory**

SUBSTRUCTURE AND MECHANICAL PROPERTIES OF TD-NICKEL

**TWO-WEEK LOAN COPY**


*This is a Library Circulating Copy  
which may be borrowed for two weeks.  
For a personal retention copy, call  
Tech. Info. Division, Ext. 5545*

**Berkeley, California**

## **DISCLAIMER**

This document was prepared as an account of work sponsored by the United States Government. While this document is believed to contain correct information, neither the United States Government nor any agency thereof, nor the Regents of the University of California, nor any of their employees, makes any warranty, express or implied, or assumes any legal responsibility for the accuracy, completeness, or usefulness of any information, apparatus, product, or process disclosed, or represents that its use would not infringe privately owned rights. Reference herein to any specific commercial product, process, or service by its trade name, trademark, manufacturer, or otherwise, does not necessarily constitute or imply its endorsement, recommendation, or favoring by the United States Government or any agency thereof, or the Regents of the University of California. The views and opinions of authors expressed herein do not necessarily state or reflect those of the United States Government or any agency thereof or the Regents of the University of California.

Rept. sub. for pub. in the  
Transactions of the American  
Institute of Mechanical Engineer-  
ing.



UCRL-11260

UNIVERSITY OF CALIFORNIA  
Lawrence Radiation Laboratory  
Berkeley, California  
AEC Contract No. W-7405-eng-48

SUBSTRUCTURE AND MECHANICAL PROPERTIES OF TD-NICKEL

M. von Heimendahl and G. Thomas

February, 1964

SUBSTRUCTURE AND MECHANICAL PROPERTIES OF TD-NICKEL

M. von Heimendahl and G. Thomas

February, 1964

Abstract

The microstructure of TD-nickel has been examined by transmission electron microscopy in the extruded, annealed and deformed states. The tensile properties have been correlated with the observed microstructures and the results are compared to those obtained from pure Ni. The important conclusions are that the thoria particles in TD-Ni act as strong barriers to dislocation motion both during deformation (slip) and annealing (climb). During deformation, the dislocations tangle around the particles and a cell structure is developed after 10% or more strain. The cell size appears to be determined by the spacing of the largest particles and is about five times smaller than that in pure nickel for the same strain. The higher work hardening rate in TD-Ni compared to Ni is probably due to the more rapid rate of dislocation multiplication in the alloy as a result of dislocation-particle interactions. The  $\text{ThO}_2$  particles inhibit recrystallization and twin growth so that some strengthening may arise from the high density of small annealing twins.

---

M. von Heimendahl on leave from the Institut für Metallkunde der Bergakademie Clausthal, Germany through a NATO Scholarship at the Department of Mineral Technology, University of California, Berkeley.

G. Thomas, Member AIME, Associate Professor of Metallurgy, Department of Mineral Technology, University of California, Berkeley.

---

## INTRODUCTION

The strengthening of materials due to the presence of a dispersed second phase has been the subject of considerable experimental and theoretical investigation in recent years. One of the newest dispersion strengthened alloys to be developed is TD-Nickel,<sup>1</sup> a system of approximately 2 vol % thoria ( $\text{ThO}_2$ ) dispersed in a matrix of commercially pure nickel. This material is fabricated by powder metallurgical techniques and offers high temperature stability and useful mechanical properties virtually to the melting point of the base metal. While the mechanical properties of this system have been investigated,<sup>2, 3</sup> there have been no reports in the literature concerning the microstructure of TD-Ni and its correlation to mechanical properties. This paper describes a transmission electron microscopy investigation of the microstructure of TD-Ni together with its mechanical properties. The results are compared to the structure and properties of pure nickel.

## EXPERIMENTAL PROCEDURE

The following states of TD-Ni have been investigated by transmission electron microscopy:

1. As-extruded material (as received).
2. Cold rolled sheet from as-extruded state.
3. Sheet annealed (after step 2) to 500°, 700°, 900° and 1200° C (annealing time 1 hr). The last two annealings were done in vacuum.
4. Deformed 2% to 10% by tensile deformation after the 900° annealing from step 3.

The sheets were all 0.25 mm thick when heat treated (i.e., before being thinned down for electron microscopy). From the as-extruded material, slices of about 0.5 mm thick were cut out perpendicular to the extrusion direction by means of a spark cutter. These slices were ground to about 0.2 mm by hand after embedding in hardening plastic. Thin foils were prepared by electropolishing in an electrolyte consisting of 35%  $H_2SO_4$ , 40%  $H_3PO_4$ , 25%  $H_2O$  at room temperature employing the window-method<sup>4</sup> with 6 V, 2-3  $A/cm^2$ , without stirring. Clean foils were obtained by this technique after the usual rinsing in distilled water followed by rinsing in ethyl alcohol. The thin foils were examined in a Siemens Elmiskop I Electron Microscope operated at an accelerating voltage of 100 kV. The tilting stage was utilized to give required contrast conditions. All rotations and inversions have been accounted for in the comparison of micrographs and selected area diffraction patterns.

Besides the electron microscopy studies, tensile experiments and grain size determinations were carried out for all the TD-Ni specimens treated as mentioned under step 3 and compared to pure nickel (99.98%) treated in identical fashion. The specimens used for electron microscopy were taken from the material used in the tensile tests. All specimens were cold rolled 90% prior to the four annealing treatments. X-ray back reflection photographs (Cu-radiation) were taken of some samples in order to check the recrystallization behavior. The grain sizes of the pure Ni samples were determined by standard metallographic methods, but the grain sizes of TD Ni samples could only be found by transmission electron microscopy done at very low magnification because

it was impossible to reveal the grainstructure by means of optical metallography. This difficulty has also been reported by other investigators and we quote from Worn and Marton.<sup>3</sup> "We have been unable to detect any grain boundaries in any of the TD-Ni alloys, using optical microscopy. A substructure was apparent in certain electron photomicrographs, but the true significance of this substructure is open to question." In the investigation described in the present paper useful pictures showing the grain structure by electron microscopy could be obtained only by using the tilting facilities to achieve suitable contrast.

## RESULTS

### A. Transmission Electron Microscopy.

Annealed Samples. Figure 1 shows the size and distribution of the ThO<sub>2</sub>-particles in one of the annealed samples (1 hr, 700°C). The particles are roughly spherical in shape and exhibit dark contrast. The size of the particles is not uniform and the diameter varies between 100 and 2000 Å. In previous investigations using carbon extraction replicas<sup>2</sup> a predominant particle size of about 0.1μ was determined. Actually as Fig. 1 shows, smaller particles are also present indicating that extraction replicas may not reveal all the particles. A detailed statistical analysis concerning the size distribution, mean planar interparticle spacing, average diameter, etc., of the particles was carried out and is described in the Appendix.

In order to prove that these particles are ThO<sub>2</sub> and not artefacts, selected area diffraction patterns were taken (Fig. 2) and analyzed. They consisted (in addition to the spot pattern of the Ni matrix) of weak, spotty rings. These rings showed a fairly uniform distribution of spots indicating



that the particles producing the rings are in random orientation. In Table I the experimental d-values obtained from patterns such as Fig. 2. are compared with the calculated first four d-values of  $\text{ThO}_2$  (cubic structure,  $a = 5.600 \text{ \AA}$ ). The agreement is good enough to prove that the rings are in fact due to  $\text{ThO}_2$  particles. Furthermore, this structure is never observed in pure nickel<sup>5</sup> (see Fig. 9). The rings appear in the typical sequence of a fcc pattern though the structure of  $\text{ThO}_2$  is more complicated. However, the contribution of the oxygen atoms to scattering is negligibly small, so that probably only the Th-atoms are responsible for the diffraction pattern.

A characteristic feature of annealed TD-nickel is the appearance of many, very narrow annealing twins, (Fig. 3): The twins are identified in the usual way by diffraction and darkfield analyses.<sup>6</sup> The boundaries of these twins are quite irregular due to the presence of the particles. This indicates that twin growth is greatly restricted due to the presence of the  $\text{ThO}_2$  particles.

For comparison, micrographs of annealed pure nickel (99.98%) were made. In no case were any annealing twins observed in the small visual field of the electron microscope. Very large twins of about 20-100  $\mu$  dia., depending on the annealing temperature, were observed under the light microscope. Thus, in TD-nickel the increased twin density due to the dispersed particles of  $\text{ThO}_2$  may also contribute to the strength.

The recrystallization behavior of TD-Ni was also studied after 90% cold work. After 1 hr at 500°C, no recrystallization could be detected. The whole sample still consisted of the cell structure typical of heavily coldworked metals of medium or high stacking fault energy (see, e.g., Fig. 10).

Table I

$d_{exp}$	$d(calc)^1$	$hkl$
3.23	3.234	111
2.79	2.800	200
1.97	1.980	220
1.69	1.689	311

(1) ASTM card index file.

The samples annealed at 700°C exhibited a mixed structure partly of recrystallized, dislocation-free, twinned areas, and partly coldworked regions (e.g., Fig. 4).

With increasing annealing temperature, the deformed areas decrease in proportion to the recrystallized areas, but even after the 1200°C anneal there were still some unrecrystallized regions visible. This was not true for pure nickel, in fact the nickel samples were fully recrystallized after the 500°C anneal. There was no difference in microstructure in the annealed regions after the 700°, 900°, 1200° C treatment. In particular the morphology of the ThO<sub>2</sub> particles is unchanged. This is in agreement with reports<sup>3</sup> that there is no coagulation of particles below 1300°C.

Plastically Deformed Specimens. Figures 5-8 show examples of microstructures from materials deformed in tension. All specimens were annealed 1 hr at 900°C before the tensile tests. In Fig. 5 the dislocation-particle interaction after 2% plastic strain can be seen. The dislocations are pinned and start to tangle around the particles. Sometimes elongated loops (A) are formed and pinned at one end at a ThO<sub>2</sub>-particle. This indicates that the dislocation line may have avoided the particle by cross-slip, leaving behind the elongated loop.<sup>7, 8</sup> These loops do not lie in the original slip plane, i.e., they are prismatic, in contrast to the concentric loops which would be left around particles if the Fisher, Hart and Pry<sup>9</sup> mechanism of dislocation-particle interaction had occurred. The latter type of loop has never been found in this investigation.

Other areas of Fig. 5 indicate possible cross slipped dislocation lines at B without a visible particle being connected. The particle

having caused the cross slip may have been too small to be resolved in this picture or may have been in the polished away portion of the specimen. Several areas show characteristic V-shaped dipoles, which may result from a pinning particle located on a glide plane. Similar defects have been observed in deformed SAP aluminum (Goodrich and Ansell, priv. comm.).

The typical pinning of long dislocation lines at the particles can be seen in Fig. 6. A significant feature in the deformation process in TD-nickel is the influence of the great number of fine-scaled annealing twins. Figure 7 is an example showing many dislocations near the twin interfaces. The density of dislocations is always higher near twin boundaries during the early stages of plastic deformation. There are examples of loops bowing from the boundaries in Fig. 7 suggesting the latter act as sources. However, with increasing deformation, due to the high dislocation density, it is not possible to distinguish whether dislocations are generated or impeded at the twin boundaries.

After larger deformations the dislocations appear to be subjected more and more to cross-slip reactions. The result is a tangled structure of dislocations leading finally to a more or less well developed cell structure. After 10% tensile deformation the cell structure is present in some, but not all areas of the samples. This is usually the case in deformed polycrystals. A typical example is shown in Fig. 8. The average cell size is determined to be about  $0.3\mu$  and this cell size is apparently governed by the spacing of the largest particles.

For comparison a sample of pure nickel (99.98%) was annealed at  $500^{\circ}\text{C}$ \* and also subjected to 10% tensile deformation. Figure 9 is only one example of many micrographs, taken in order to determine the cell size in this case.

---

\* This temperature was found to yield a completely recrystallized but fine grained pure Ni. See also Table II.

---

Table II. Summary of Tensile Tests and Grain Size Analyses.

Material	Annealing Treatment	1hr-500°C	1hr-700°C	1hr-900°C	1hr-1200°C
	Property				
99.98% Ni 90% coldrolled and annealed	Yield Stress (kg/mm <sup>2</sup> )	4.65	2.7	2.4	1.8
	Average Grain-size (μ)	25	55	75	125
TD-Ni 90% coldrolled and annealed	UTS (kg/mm <sup>2</sup> )	72	56.5	55.3	50.7
	Flow Stress $\sigma_{0.01}$	55	35	23	23
	$\sigma_{0.1}$	63	39	29	28
	Average Grain-size (μ) of re-crystallized areas	Not re-crystallized	5-11	5-11	5-11
	Percentage of re-crystallized areas	0	40-60	70-90	99

Here the cell character is fairly well developed and the average cell size was determined to be  $1.5\mu$  with a minimum value of  $0.5\mu$  and a maximum value of  $3\mu$ . This result agrees with previous cell structure investigations of Nolder and Thomas.<sup>5</sup> Finally, the structure of TD-Ni cold rolled after 90% reduction in thickness is shown in Fig. 10. The cell structure is now much more pronounced as compared to Fig. 8.

As-extruded State. Figure 11 represents an example of the as-extruded structure showing a section perpendicular to the direction of extrusion. Here the grain size is remarkably small (about  $1\mu$ ). Small angle dislocation boundaries as well as large angle boundaries are present. Furthermore, there are dislocations inside many of the grains due to the severe cold-work involved in the extrusion process. Hence, recrystallization during the hot extrusion is not effective in eliminating these dislocations.

#### B. Mechanical Tests and Comparison with 99.98% Nickel.

The tests described in the following were made in order to investigate the mechanical behavior in comparison with the microstructure as a function of annealing temperature, i.e., grain size. Firstly, to check the beginning of the recrystallization, x-ray back reflection photographs were taken. By this it was recognized that the pure nickel was completely recrystallized after 1 hr at  $500^{\circ}\text{C}$ . On the other hand, any recrystallization of the TD-Ni which was revealed by transmission micrographs could not be detected by standard x-ray back reflection techniques since the grain size was so small. Even after the annealing treatment at  $1200^{\circ}\text{C}$ , the Debye-Scherrer rings were completely homogeneously blackened and not spotty. Faint rings according to the  $\text{ThO}_2$  could be recognized on all TD-Ni x-ray photographs; the matrix rings have the typical appearance of a strong texture.

The results of the tensile tests are shown in Fig. 12. Table II summarizes the data of interest concerning the samples. Figure 13 gives a summarizing plot of the observed flow stresses (0.1% offset) against the inverse square root of the grain sizes. The scatter in the grain sizes of TD-Ni is considerable since the grain sizes vary widely. There was no significant change in the grain sizes of the recrystallized areas after annealing at 700°, 900° or 1200° C. One example of the many low magnification transmission micrographs taken in order to determine the grain size is shown in Fig. 14. The higher values of  $\sigma_{0.1}$  for TD-Ni at 500° and 700° C are certainly due to the fact that the material was not completely recrystallized, but it seems remarkable that the yield stress as well as the ultimate tensile stress after 1 hr 500°C is considerable higher than those previously reported.<sup>2</sup> The reason for this result is unknown.

The results from the investigations of the pure nickel specimens showed the well known linear relationship between (grain size)<sup>-1/2</sup> and yield stress, (the so-called Petch relationship<sup>10, 11</sup>), whereas in the case of TD-Ni; since the grain size was found to be relatively invariant with annealing treatment (in the investigated temperature range), no such relationship was found.

## DISCUSSION

From the results of this investigation, the hardening mechanism in the case of TD-Ni may be described as the following. At stresses close to the yield stress, the dislocation lines may move but are quickly pinned by the  $\text{ThO}_2$ -particles and bow out between them according to the amount of the acting shear stress (e.g., see Fig. 6). This is in qualitative agreement with the Orowan-mechanism.<sup>12</sup> With increasing stress beyond the yield stress, however, the dislocations obviously do not bow around the particles completely, neither are concentric loops left behind as predicted by some theories.<sup>9, 12</sup> Rather, the dislocations cross slip, as expected in metals of medium or high stacking fault energy, and tangle around the particles. It is probable that during cross slip dislocation multiplication occurs and this gives rise to a localized increase in dislocation density around the particles.

Finally the formation of a cell structure occurs in TD-Ni as well as in pure nickel. But in TD-Ni the formation of cells is obviously retarded by the presence of the particles, e.g., after 10% tensile strain the cell structure is much less pronounced in TD-Ni than in pure Ni (compare Figs. 8 and 9). The cell size in TD-Ni seems to be governed by the particle spacing, the large particles often were found to act as "corner posts" for the cells. On the other hand, TD-Ni has a higher work hardening rate than pure Ni (Fig. 12) and this may be attributed to the larger dislocation density due to dislocation-particle interactions with increasing strain. Furthermore, the large number of annealing twin boundaries in TD-Ni may act as preferred sites for dislocation nucleation (e.g., Fig. 7), on the other hand they also act as barriers to moving dislocations. Hence, some strengthening



may also be effected by the high twin density.

Intersection of the  $\text{ThO}_2$ -particles by dislocations was never observed. This is expected because of the refractory nature of  $\text{ThO}_2$ . Particles of this type which are larger than about  $10 \text{ \AA}$  will not be sheared by dislocations.<sup>12, 13</sup>

With regard to the mechanical tests, the most striking effect is the stability of the structure even after annealing at temperatures as high as  $1200^\circ\text{C}$ . The grain size is very small and is the same for recrystallization at  $700^\circ$  as well as  $1200^\circ \text{C}$ . This structure, its stability and the high yield stress, is certainly due to the presence of the  $\text{ThO}_2$  particles. The particles inhibit not only grain growth but recrystallization generally: in all TD-Ni samples unrecrystallized areas of high dislocation density were observed even after the  $1200^\circ\text{C}$  anneal. All the processes involved in recovery and recrystallization, e.g., motion of dislocation by climb are obviously strongly inhibited. In the 99.98% pure Ni sample, for comparison, recrystallization started as low as a  $300^\circ\text{C}$  and was found to be completely finished at about  $400^\circ\text{C}$  for an initial 90% cold work.

The mechanical tests as a function of annealing temperature and grain size were done originally on TD-Ni in order to find out whether there is a yield stress - grain size or a yield stress - particle spacing relationship. However, as shown in Fig. 13 no grain size effect is observed. Concerning the effect of the particles the following may be remarked. The initial yield stress in the case of non-deforming particles is given by the extended Orowan-relationship<sup>14</sup>

$$\tau = \tau_s + \frac{Gb}{4\pi} \phi \ln \left( \frac{d-2r}{2b} \right) \frac{1}{(d-2r)/2} \quad [1]$$

$$\begin{aligned}
 G &= \text{shear modulus of matrix} && = 7000 \text{ kg/mm}^2 \\
 b &= \text{burgers vector} && = 2.5 \times 10^{-7} \text{ mm} \\
 r &= \text{mean particle radius} && = 2.0 \times 10^{-5} \text{ mm (see Appendix)} \\
 d &= \text{mean planar interparticle spacing} && = 0.28 \times 10^{-3} \text{ mm (see Appendix)} \\
 \tau_s &= \text{initial yield stress of matrix} && \approx 0.7 \text{ kg/mm}^2 \text{ (Haasen}^{15}) \\
 \phi &= \frac{1}{2} \left( 1 + \frac{1}{1-\nu} \right), \quad \nu = \text{Poisson's ratio.} && \phi \approx 1.25
 \end{aligned}$$

Using the above values we obtain  $\tau = 10.0 \text{ kg/mm}^2$ . However, any test of the Orowan-relationship can only be done using single crystals (in this case  $\tau$  represents the critical resolved shear stress), since in the case of polycrystals the grain boundaries are an additional complicating factor. As yet there is no theory delivering a relationship for the yield stress of two-phase polycrystals as a function of particle spacing, grain size, etc., so we may consider the value of  $10.0 \text{ kg/mm}^2$  from equation [1] only as a lower limit. The actual shear stresses of the (nearly) fully recrystallized polycrystalline samples are about 50% higher, assuming that the tensile yield stress (Fig. 12) in polycrystals ( $\sim 30 \text{ kg/mm}^2$ , from Table II) is about twice the shear stress. This is certainly due to the additional contribution of the grain boundaries, twin boundaries and effects associated with preferred orientation. To check equation [1] correctly, experiments with TD Ni single crystals would be very desirable; however, the difficulties of making such crystals are great.

#### ACKNOWLEDGMENTS

This research was possible through a NATO scholarship (German Academic Exchange Service) to M. vH. and through continued support by the U. S. Atomic Energy Commission through the Inorganic Materials Research Division of the Lawrence Radiation Laboratory, University of California, Berkeley. The materials were kindly donated by Drs. J. White and R. D. Carnahan of Aerospace Corporation. We also thank Dr. R. S. Goodrich for valuable discussions and for making the results of a similar investigation on SAP aluminum available prior to publication.

## APPENDIX

A statistical analysis concerning the particles was carried out as follows. The particles visible in areas of  $1\mu^2$  of the electron micrographs were counted and their individual diameters measured. There were, e.g.,  $130 \pm 10$  particles per square micron of view. Since the particles are spherical in shape the total volume sum of all these particles can be calculated. The knowledge that 2 vol. % thoria are present enables furthermore a calculation of the foil thickness to be made, since 100 vol. % represents a volume of  $1\mu^2$  area times foil thickness  $t$ . For example, in Fig. 1,  $t$  is 2300 Å. The particle density,  $N_v$ , was determined to be 555 particles/ $\mu^3$ . This number and the known volume fraction (0.02) of dispersed phase allow a determination to be made of the data given in table III, using the notation and methods given by Underwood.<sup>16</sup> The distribution of all particles vs. size reveals that there is a maximum in size distribution between 100 and 200 Å diameter, but the major contribution to the whole volume of the dispersed phase is from the few large particles of more than 1000 Å diameter. It should be emphasized as pointed out by Kelly and Nicholson,<sup>14</sup> that the quantity  $d$  in the Orowan-relationship (equation [1]) is the mean planar interparticle spacing and not the mean free path  $\lambda$ . This mean planar interparticle spacing,  $d$ , can be found using the relation<sup>17</sup>  $4r^2/d^2 = f$  where  $f$  is the volume fraction of the second phase and  $r$  is the mean planar particle radius. As shown in the last row of Table III, the value for  $d$  is consistently  $\sim 0.28\mu$  in TD-Ni.

Table III

		<u>Sample A</u>	<u>Sample B</u>	<u>Sample C</u>	<u>Average of Sampling</u>
No. of particles/ $\mu^3$	$N_V =$	740	555	670	655
No. of particles/ $\mu^2$	$N_A =$	28	23	25	25
No. of particles/ $\mu$	$N_L =$	0.80	0.73	0.76	0.76
Mean center-to-center-distance in $\mu$	$1/N_L = S_p =$	1.25	1.37	1.31	1.31
Mean free path in $\mu$	$S_p - D = \lambda =$	1.21	1.33	1.27	1.27
Average particle diameter in $\text{\AA}$	$2r = D_{av} =$	380	400	400	393
Mean planar interparticle spacing in $\mu$	$d =$	0.27	0.28	0.28	0.28

The Table contains the results of three independent analyses from different samples in the three columns. The values from the last column represent average values.

REFERENCES

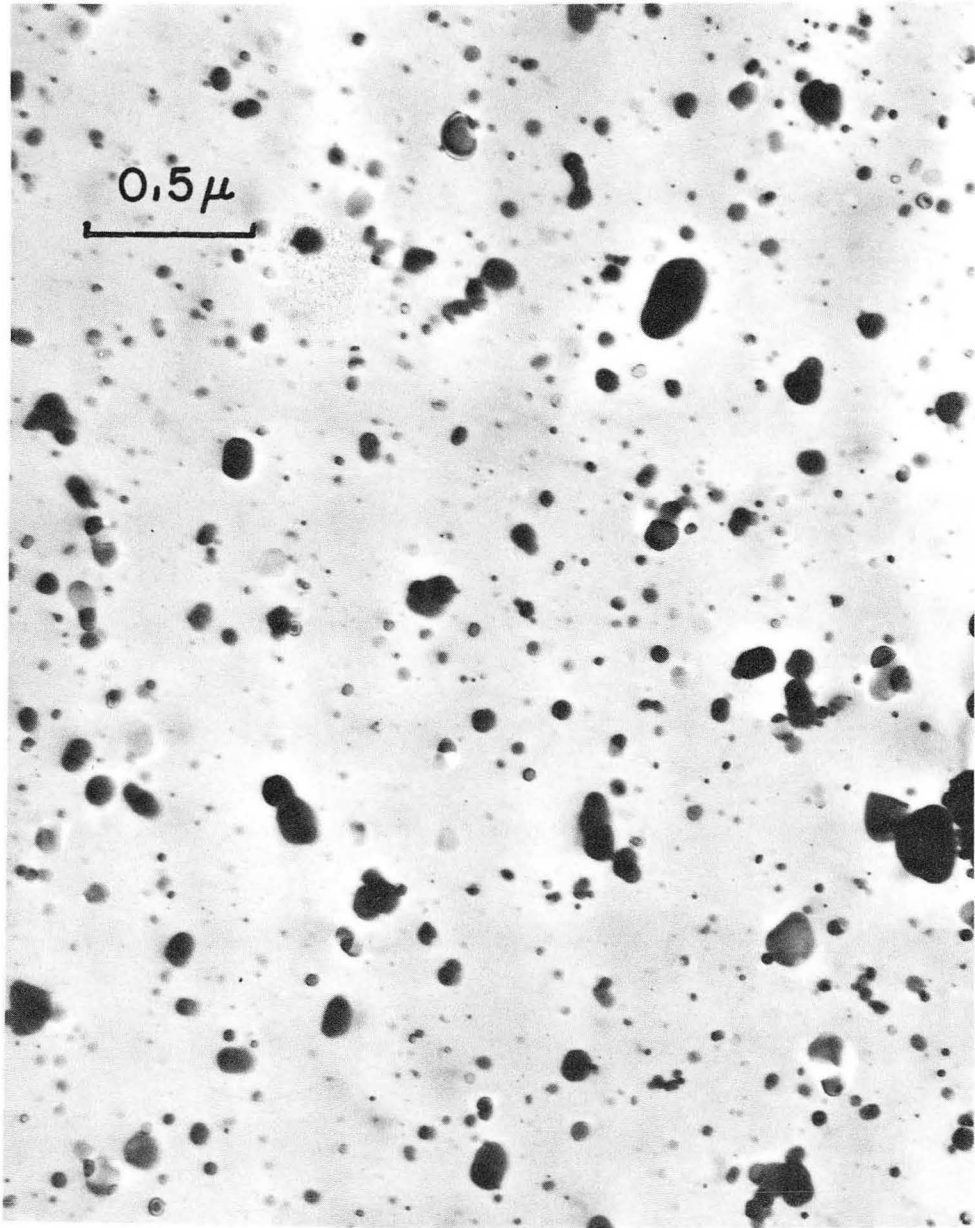
- <sup>1</sup> Du Pont Metal Products.
- <sup>2</sup> F. J. Anders, G. B. Alexander and W. S. Wartel, *Metal Progress*, 1962, vol. 82, p. 88.
- <sup>3</sup> D. K. Worn and S. F. Marton, Powder Metallurgy, p. 309, Interscience Publishers, New York, 1961.
- <sup>4</sup> G. Thomas, Transmission Electron Microscopy of Metals, J. Wiley & Sons Publishers, New York, 1962.
- <sup>5</sup> R. L. Nolder and G. Thomas, *Acta Met.*, 1963, vol. 11, p. 994.
- <sup>6</sup> O. Johari and G. Thomas, *Trans AIME*, 1964, in press.
- <sup>7</sup> P. B. Hirsch, G. Thomas and J. Nutting, *J. Inst. Metals*, 1957-58, vol. 86, p. 7.
- <sup>8</sup> M. F. Ashby, Electron Microscopy and Strength of Crystals, p. 896, Ed. by G. Thomas and J. Washburn, Interscience Publishers, New York, 1963.
- <sup>9</sup> J. C. Fisher, E. W. Hart and R. H. Pry, *Acta Met.*, 1953, vol. 1, p. 336.
- <sup>10</sup> N. J. Petch, *J. Iron and Steel Inst.*, 1953, vol. 174, p. 25.
- <sup>11</sup> A. Cracknell and N. J. Petch, *Acta Met.*, 1955, vol. 3, p. 186.
- <sup>12</sup> See e.g., A. Kelly, Electron Microscopy and Strength of Crystals, p. 947, Ed. by G. Thomas and J. Washburn, Interscience Publishers, New York, 1963.

- 13 L. I. van Torne and G. Thomas, *Acta Met.*, 1963, vol. 11, p. 881.
- 14 A. Kelly and R. B. Nicholson, *Precipitation Hardening, Progress in Materials Science*, Ed. by Bruce Chalmers, 1963, vol. 10, p. 151.
- 15 P. Haasen, *Phil. Mag.*, 1958, vol. 3, p. 384.
- 16 E. E. Underwood, *J. Inst. Metals*, 1963-64, vol. 92, p. 124.
- 17 M. F. Ashby, *Ph.D. Thesis, Cambridge University*, 1961.

FIGURE CAPTIONS

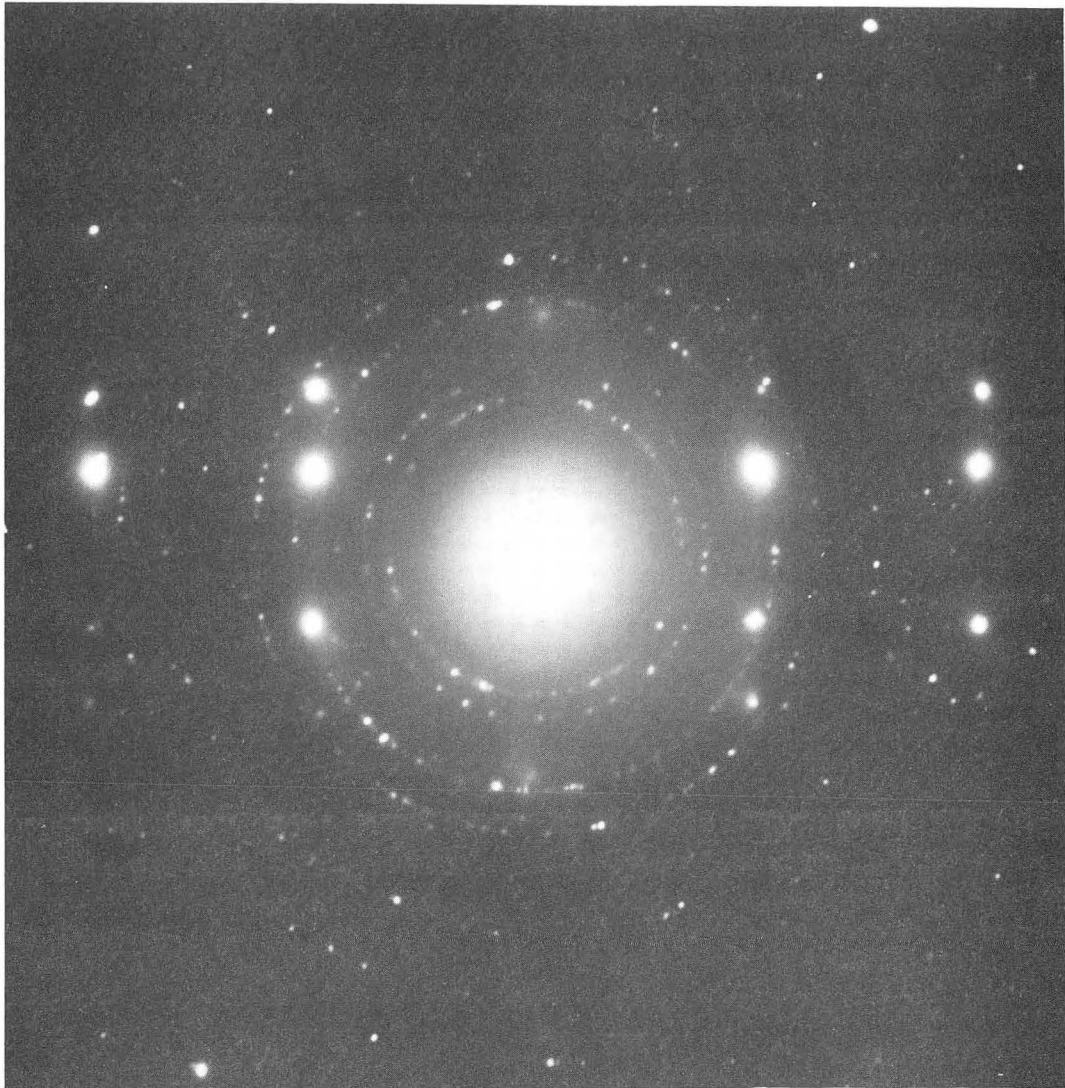
- Fig. 1. TD-Ni annealed at 700°C for 1 hr.
- Fig. 2. Typical diffraction pattern of TD-Ni. Notice the twin related spots from the matrix.
- Fig. 3. TD-Ni showing annealing twins (1hr, 700°C).
- Fig. 4. TD-Ni 1hr, 700°C annealed. Typical picture showing partial recrystallization.
- Fig. 5. TD-Ni annealed 900°C, 2% tensile strain showing tangling of dislocation around particles.
- Fig. 6. TD-Ni annealed 900°C, 2% tensile strain showing pinning of long dislocation lines.
- Fig. 7. TD-Ni annealed 900°C, 2% tensile strain showing possible dislocations from twin boundaries.
- Fig. 8. TD-Ni annealed 900°C, 10% tensile strain showing early stages of cell formation.
- Fig. 9. 99.98% pure nickel annealed 500°C, 10% plastic strain showing well developed cell structure.
- Fig. 10. TD-Ni, 90% cold rolled from extruded bar.
- Fig. 11. TD-Ni, as-extruded; the section is perpendicular to the extrusion direction.
- Fig. 12. Stress strain curves of TD-Ni and pure Ni.
- Fig. 13. Summarizing plot of flow stress (0.1% offset) vs. (grain size)<sup>-1/2</sup>.
- Fig. 14. TD-Ni annealed 1hr, 700°C low magnification micrograph such as is used for grain size determinations.





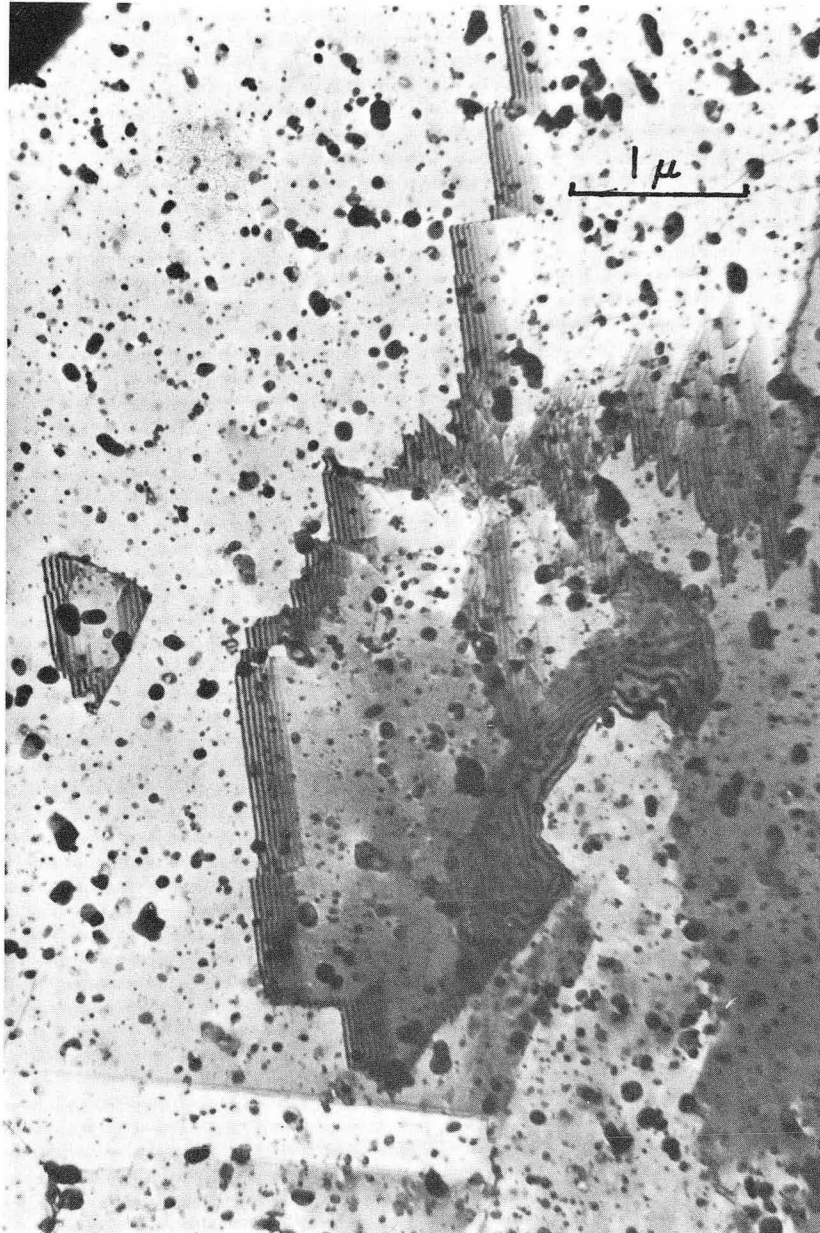
ZN-4216

Fig. 1.



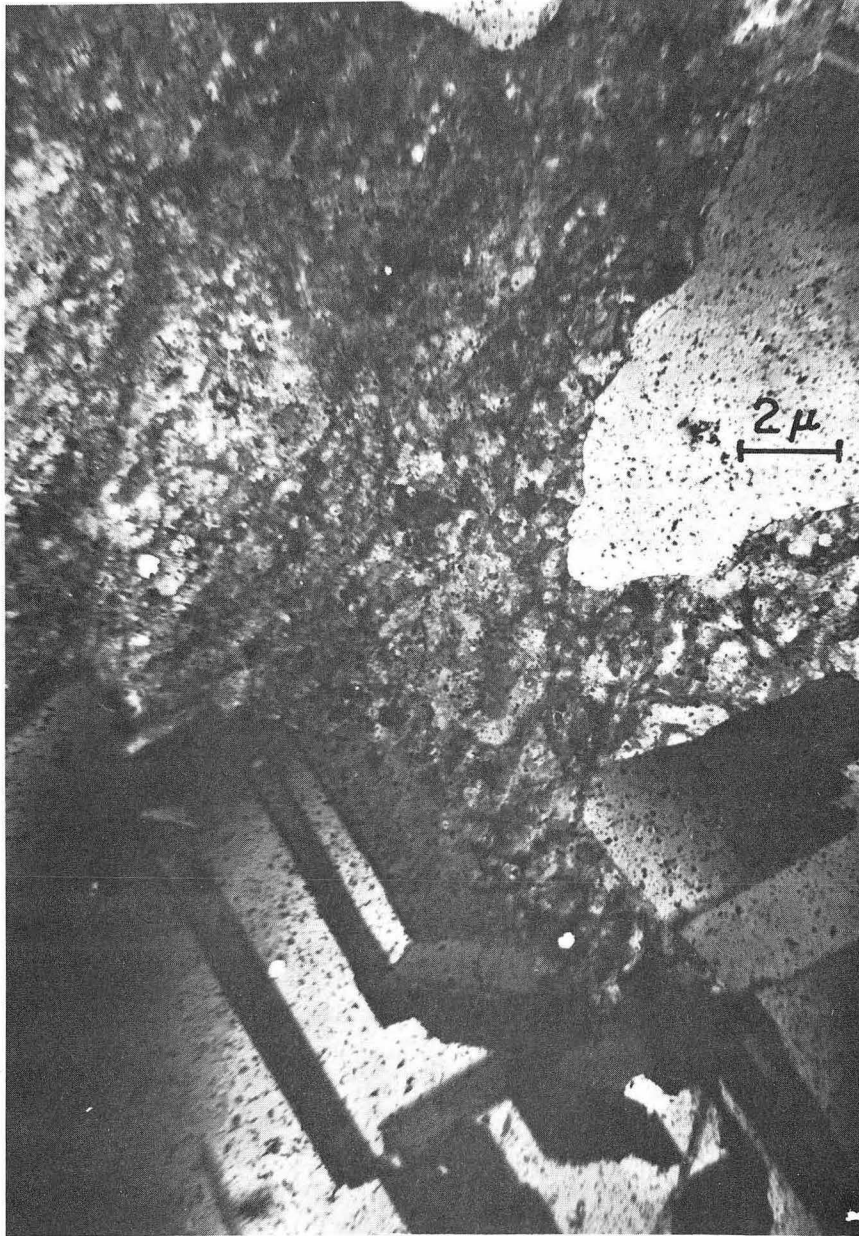
ZN-4205

Fig. 2.



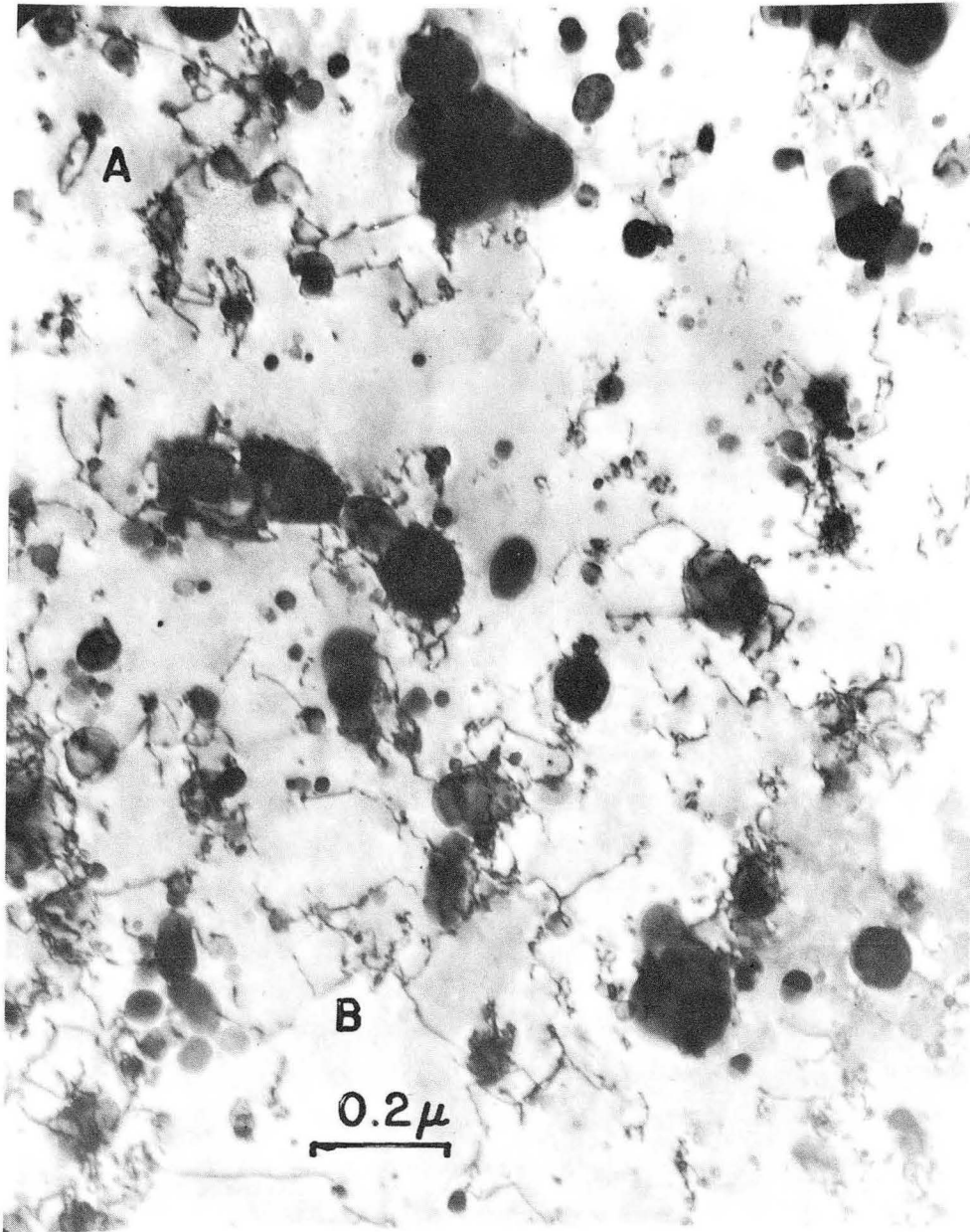
ZN-4206

Fig. 3.



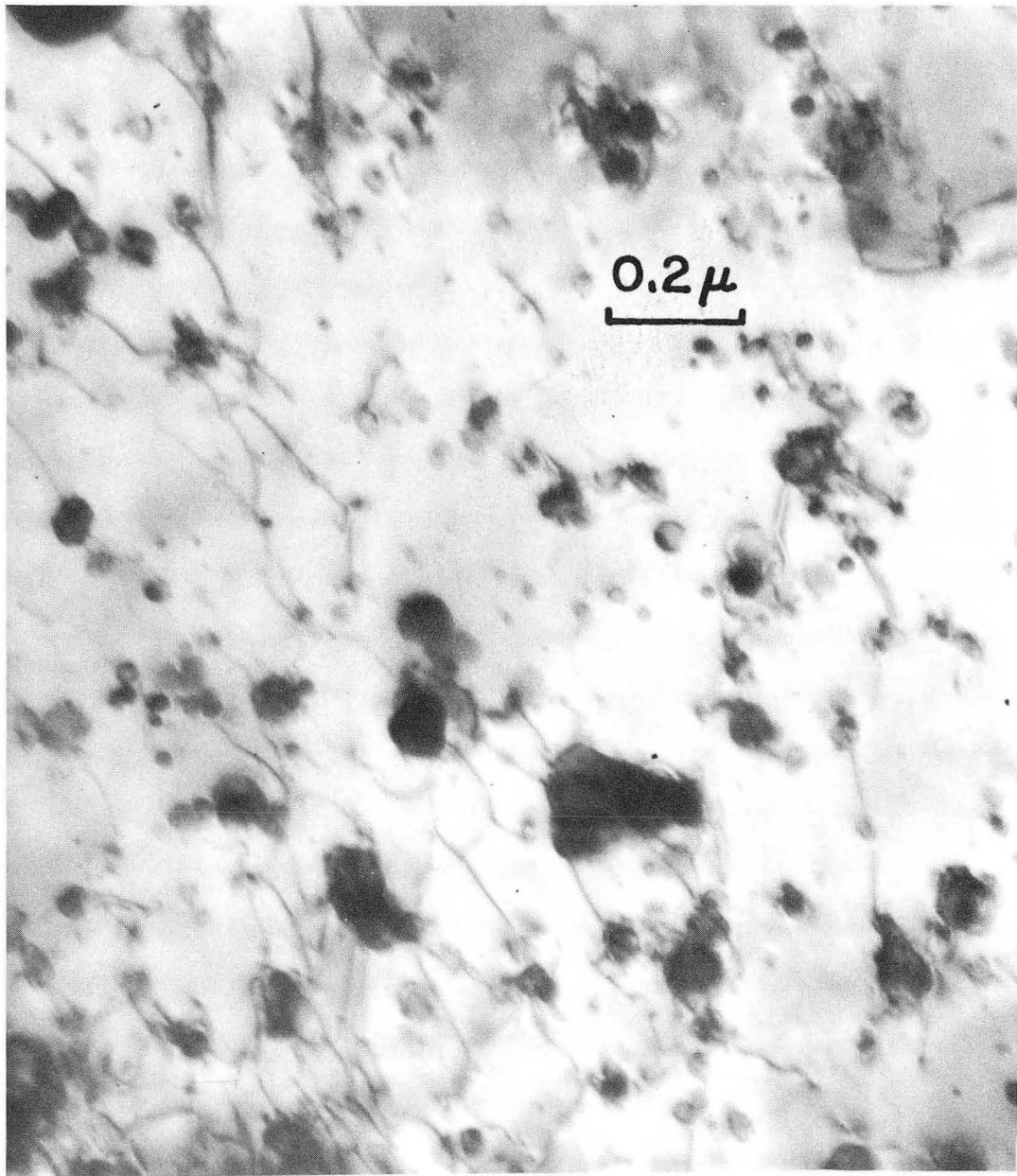
ZN-4207

Fig. 4.



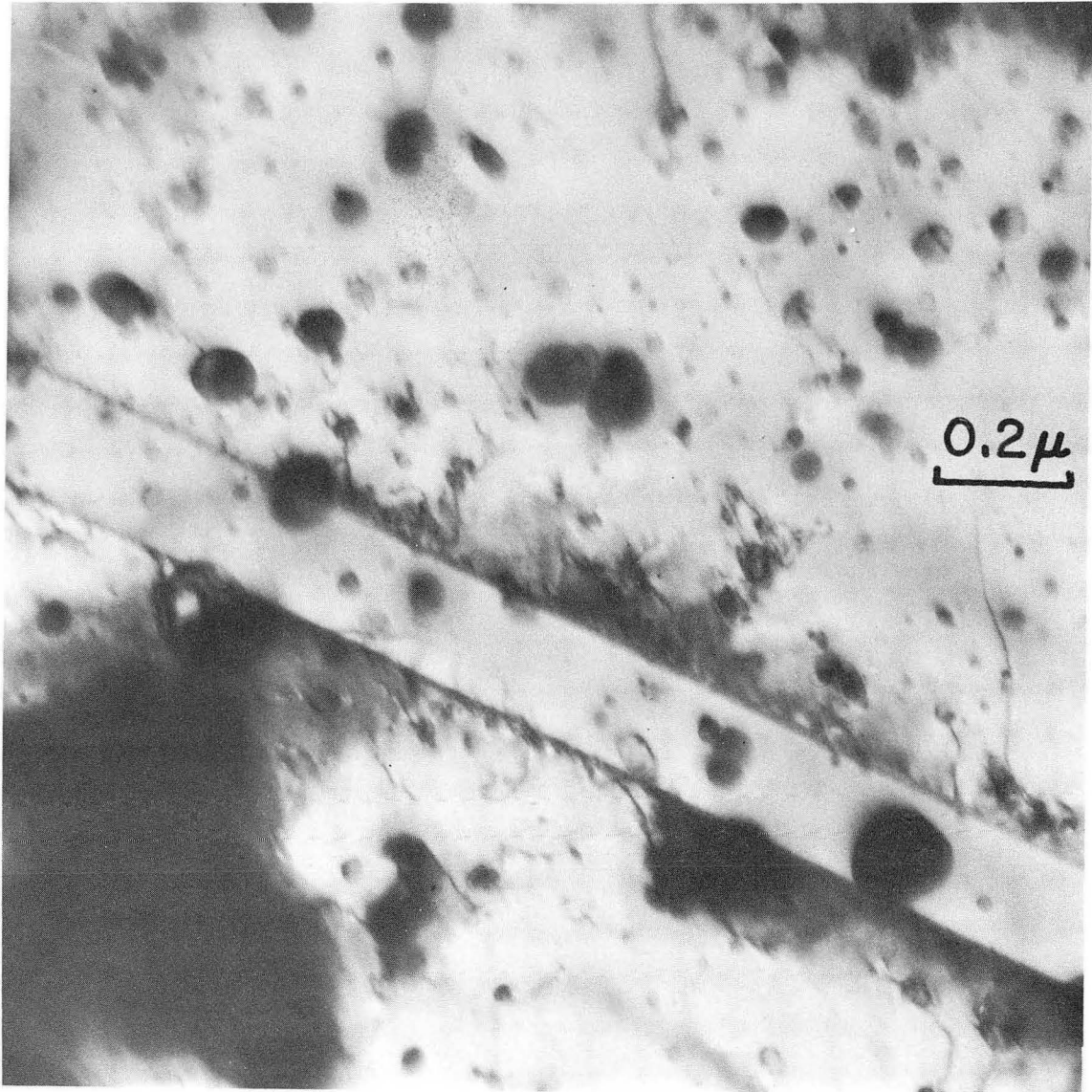
ZN-4208

Fig. 5.



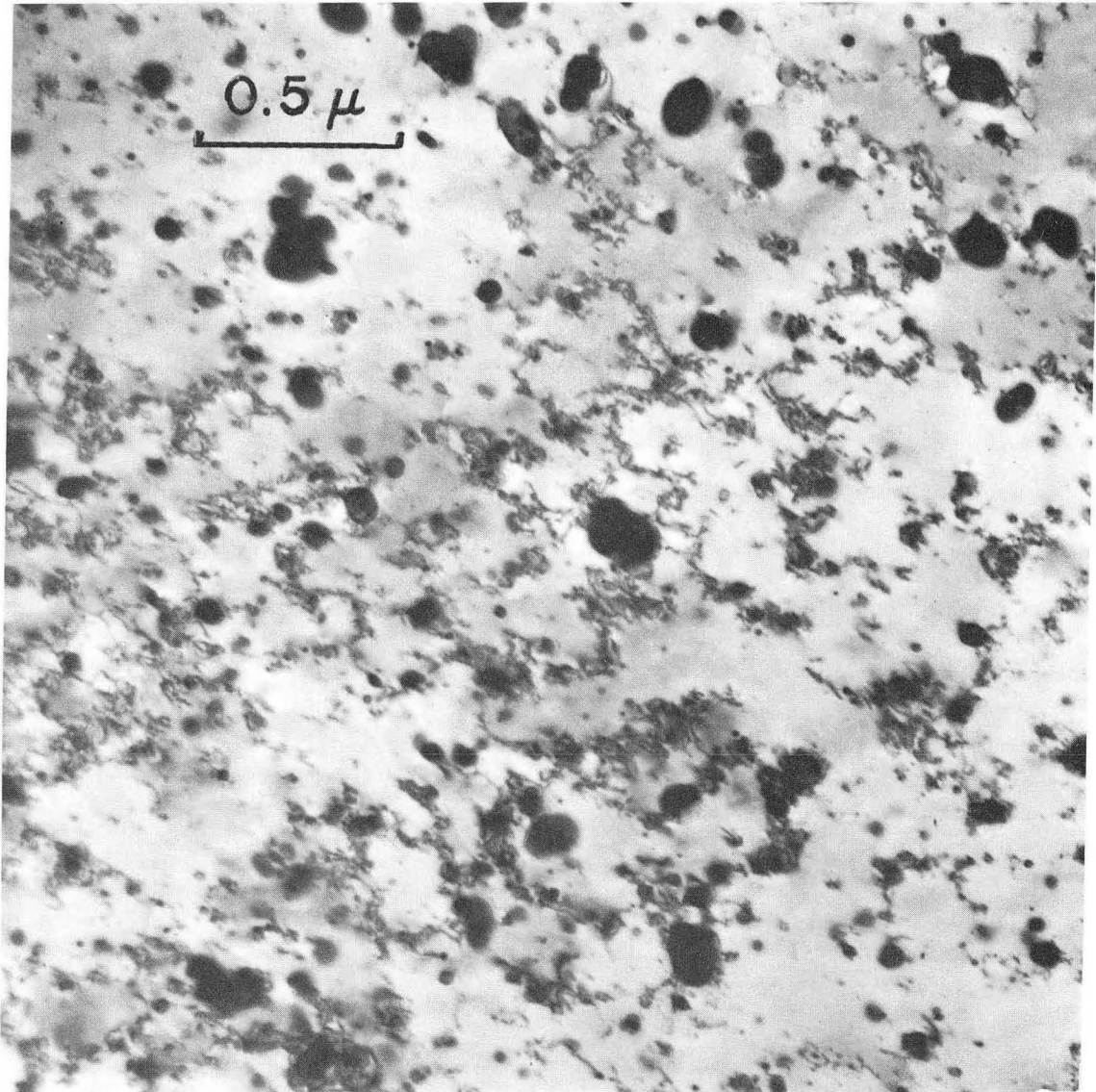
ZN-4209

Fig. 6.



ZN-4210

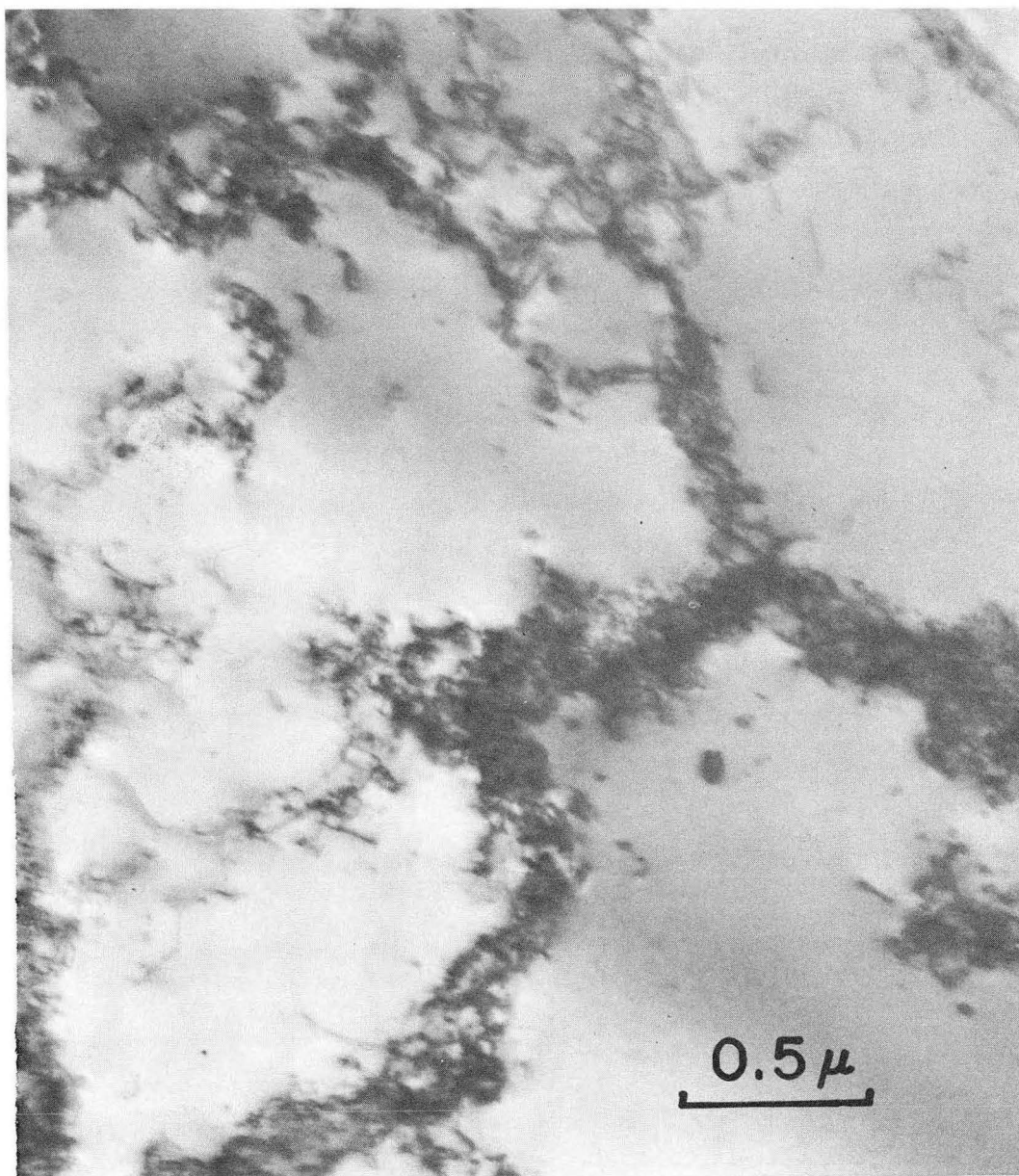
Fig. 7.



ZN-4211

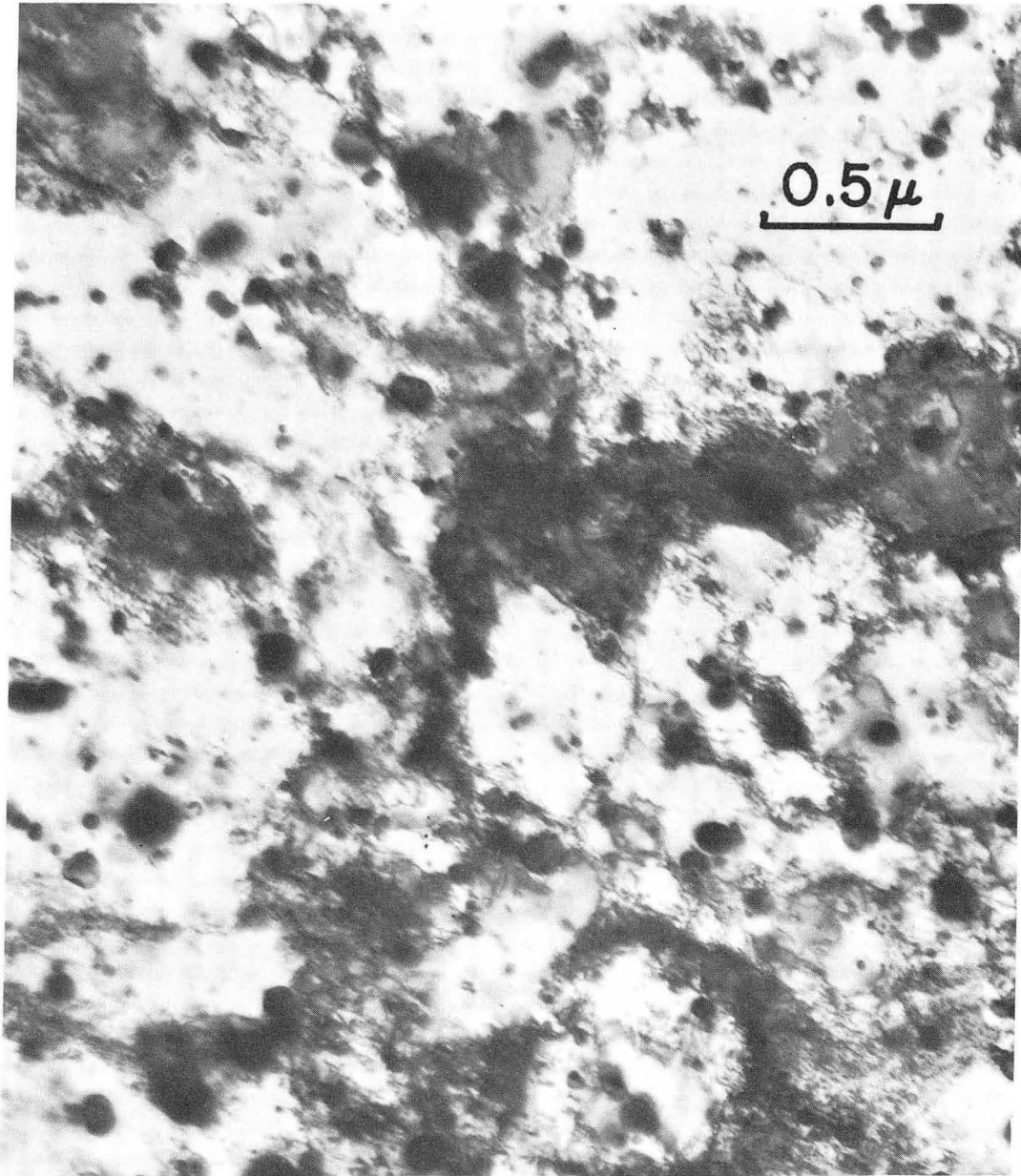
Fig. 8.





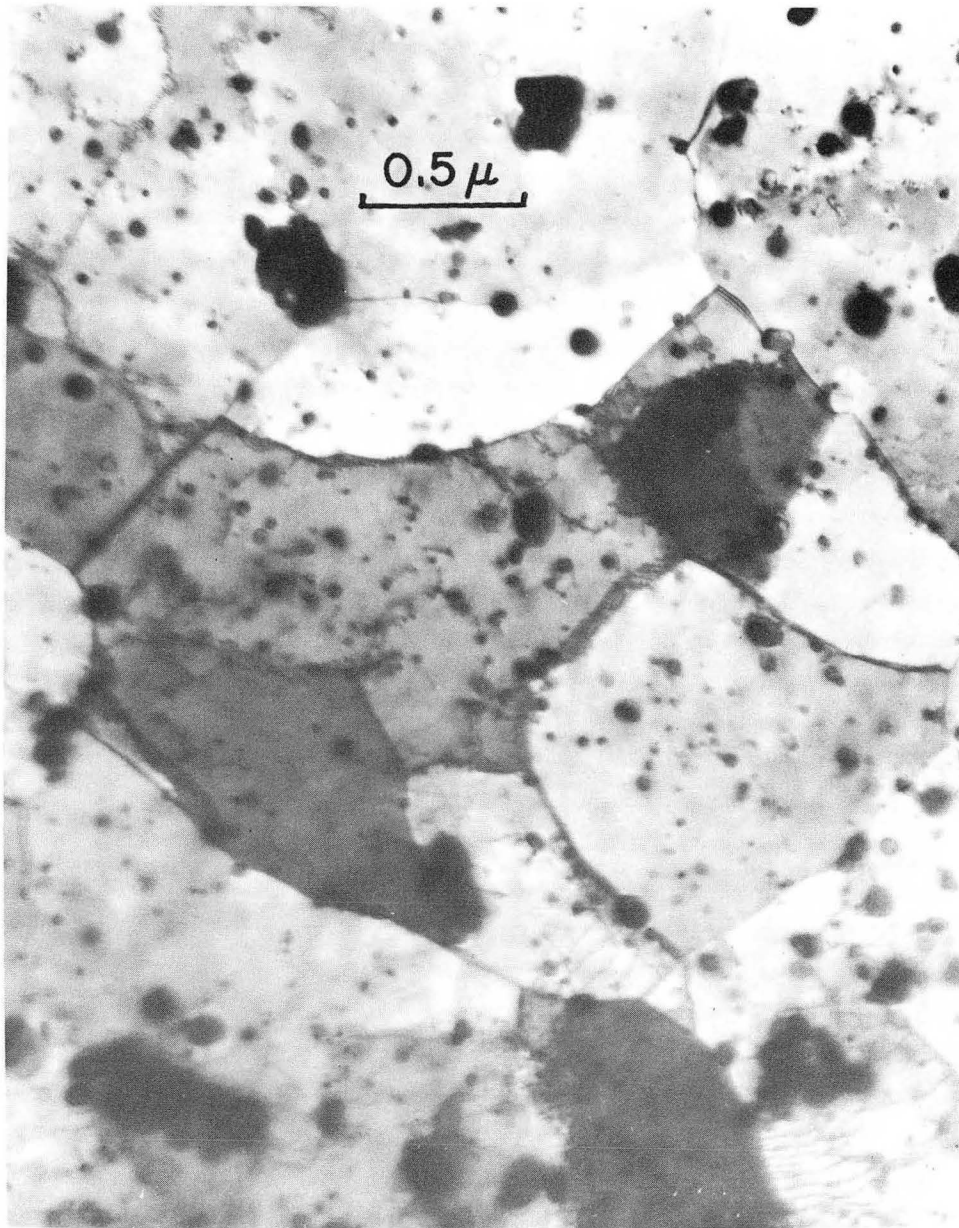
ZN-4212

Fig. 9.



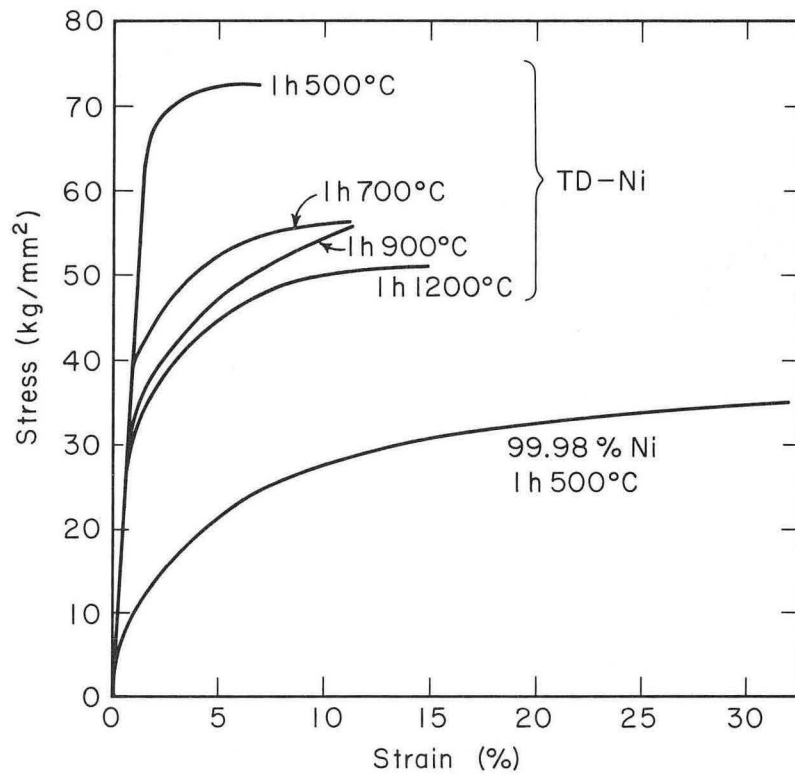
ZN-4213

Fig. 10.



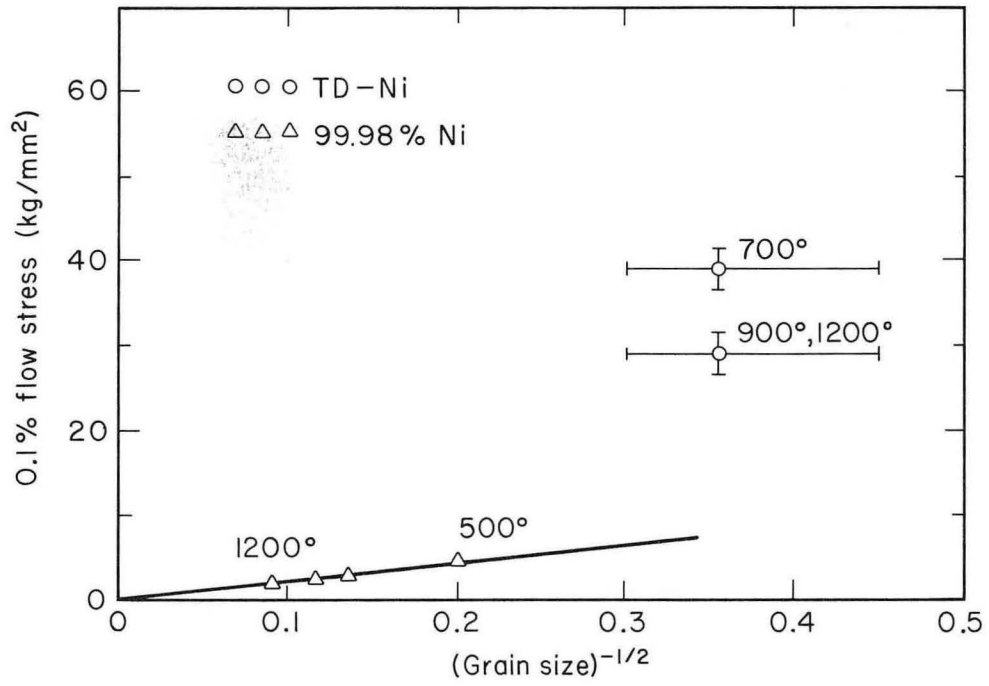
ZN-4214

Fig. 11.



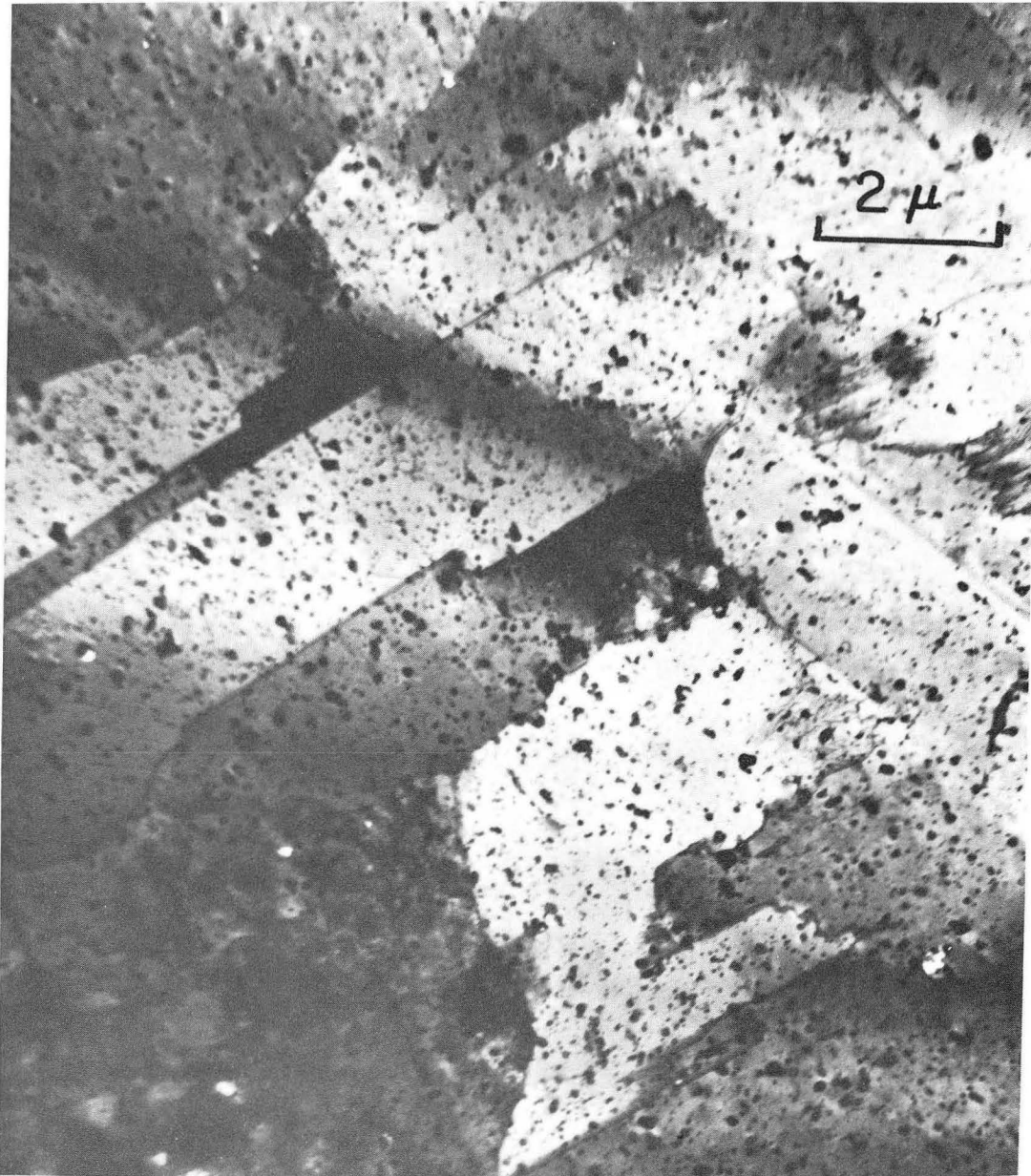
MU-33302

Fig. 12.



MU-33301

Fig. 13.



ZN-4215

Fig. 14.

This report was prepared as an account of Government sponsored work. Neither the United States, nor the Commission, nor any person acting on behalf of the Commission:

- A. Makes any warranty or representation, expressed or implied, with respect to the accuracy, completeness, or usefulness of the information contained in this report, or that the use of any information, apparatus, method, or process disclosed in this report may not infringe privately owned rights; or
- B. Assumes any liabilities with respect to the use of, or for damages resulting from the use of any information, apparatus, method, or process disclosed in this report.

As used in the above, "person acting on behalf of the Commission" includes any employee or contractor of the Commission, or employee of such contractor, to the extent that such employee or contractor of the Commission, or employee of such contractor prepares, disseminates, or provides access to, any information pursuant to his employment or contract with the Commission, or his employment with such contractor.

